Extreme flood events reconstruction spanning the last century in the El Bibane lagoon (Southeast of Tunisia): a multi-proxy approach

A. Affouri[a,b], L. Dezileau[b] and N. Kallel[a]

a : Laboratoire Georessources, Matériaux, Environnements et changements globaux, LR13ES23 (GEOGLOB), Faculté des Sciences de Sfax, BP1171, Sfax 3000, Université de Sfax, Tunisie.

b : Geosciences Montpellier, CNRS/INSU, UMR 5243, Université Montpellier, Montpellier, France.

Corresponding authors: **aidaemna@yahoo.fr (***A. Affouri*) and **dezileau@gm.univ-montp2.fr** (*L. Dezileau*)

Abstract

Climate models project that rising atmospheric carbon dioxide concentrations will increase the frequency and the severity of some extreme weather events. The flood events represent a major risk for populations and infrastructures settled on coastal lowlands. Recent studies of lagoon sediments have enhanced our knowledge on extreme hydrological events such as paleo-storms and on their relation with climate change over the last millennium. However few studies have been undertaken to reconstruct past flood events from lagoon sediments. Here, the past flood activity was investigated using a multi-proxy approach combining sedimentological and geochemical analysis of surfaces sediments from the Southeast of Tunisia catchment in order to trace the origin of sediment deposits in the El Bibane lagoon. Three sediment sources were identified: marine, aeolian, and fluvial. When applying this multi-proxy approach on the core BL12-10, recovered from the El Bibane lagoon, we can see that finer material, high content of the clay and silt, and high content of the elemental ratios (Fe/Ca and Ti/Ca) characterize the sedimentological signature of the paleoflood levels identified in the lagoonal sequence. For the last century which is the period covered by the

BL12-10 short core, three paleo-flood events were identified. The age of these flood events have been determined by ^{210}Pb and ^{137}Cs chronology and give age of AD 1995 ± 6, AD 1970 ± 9 and AD 1945 ± 9. These results show a good temporal correlation with historical flood events recorded in the Southern of Tunisia in the last century (A.D 1932, A.D 1969, A.D 1979 and A.D 1995). Our finding suggests that reconstruction of the history of the hydrological extreme events during the upper Holocene is possible in this location, by the use of the sedimentary archives.

Keywords: El Bibane Lagoon; watershed basin; surface sediments; geochemistry; grain size; paleo-floods, upper Holocene, Southeast Tunisia.

1. Introduction

The Mediterranean region has experienced numerous extreme coastal events, such as flood events which caused casualties and economic damages (Lionello et al., 2006). However, the meteorological instrumental records are limited to only a few decades, especially in Southern Mediterranean countries. Geological data offer a way to reconstruct the historical records of intense flood events. Deciphering records of extreme precipitation and damaging floods preserved in geologic archives enables society to understand and plan for floods in the future (Parris et al., 2009). The importance of studying trees, river and lake sediments has already been shown for reconstructing extreme flooding events (Baker, 1989; Ely et al., 1993; Brown et al., 2000; Benito et al., 2003; Wolfe et al., 2006; Moreno et al., 2008; Wilhelm et al., 2012; St. George and Nielsen, 2003; Gilli et al., 2013). Few studies have been undertaken to reconstruct past flood events from lagoon sediments (Raji, 2014). Most of the studies were interested to flooding associated with both hurricanes and tsunamis where overwash deposits are preserved within back-barrier lagoons and salt ponds can provide a mean for documenting previous flooding activity (Liu & Fearn, 1993; Donnelly and Woodruff, 2007; Sabatier et al., 2008; Dezileau et al., 2011, 2016; Raji et al., 2014, Degeai et al., 2015). Heavy rain flooding

events recorded within these lagoon environments are still poorly documented. Moreover, reconstruction of past flood events from sedimentary archives has been poorly studied in Southern Tunisia. Zielhofer et al. (2004) have used fluvial archives to reconstruct past fluvial activity in the northern part of Tunisia. In this study we tried to reveal the importance of lagoonal archives to reconstruct past flood activities under a semi-arid environment in southern part of Tunisia, studying the paleo-floods from high resolution geochemical and sedimentogical analyses. The first aim of this study was to identify the different sediment sources and to retrace the marine, the fluvial and the aeolian contributions to the sedimentation in the El Bibane Lagoon. The second aim was to reconstruct flood events from the lagoonal archives during the last century. To reach these objectives, we undertook the calibration of the sedimentological and geochemical proxy data with historical flood records.

2. Study site: El Bibane Lagoon and its watershed

Morphologically, southern Tunisia known as the Tunisian platform includes two distinguished morpho-tectonic domains (Fig. 1) namely: The Djeffara (Inner domain) and the Dahar (Outer domain). The Djeffara extends over all the coastal plain from Gabes (Southeastern Tunisia) to the Libyan borders. It is limited to the west by the Matmata and the Dahar mountains and to the east by the Gulf of Gabes and the Mediterranean Sea. The Dahar belongs to the Saharan platform domain is constituted by successions sequences ranging in age from the Late Permian to the Late Cretaceous (Fig.1B). The lithostratigraphic successions could be summarized as following: The Early–Middle Triassic sequence in the Dahar plateau is mainly constituted by continental sandstone, conglomerate and clay; whereas the Late Triassic outcrops exhibit shallow marine carbonate (Busson, 1967). The Jurassic series are represented by a thick Liassic evaporitic sequence, Dogger marine carbonate and late Jurassic–Neocomian mixed facies with continental predominance (Bouaziz et al., 2002). The Cretaceous series represents a general succession from neritic, lagoonal and continental facies

(Mejri et al., 2006). The Late Cretaceous is characterized by thick shallow marine carbonates-marl sequences and covered by sand dunes of the Eastern Saharan Erg.

The Mio-Pliocene series represent the substratum of the coastal plain of Djeffara. Jedoui et al. (1998) subdivided these series into two principal facies: (1) the red coloured clays rich in gypsum and (2) the sands which locally associated with conglomerates and grey clays. The Pleistocene marine deposits of the Southeast Tunisian coastal zone assigned to the "Tyrrhenian" (under marine isotopic stage 5e: last interglacial) overly unconformably the Mio-Pliocene. These deposits form a ridge parallel to the actual coast. They show the superposition of two units described by Jedoui et al. (2002) as the lower "quartz-rich unit" and the upper "carbonate unit" with *Strombus bubonius*.

The study area is focused on the El Bibane Lagoon and its watershed (El Bibane Lagoon: 33° 15' 01"N-11° 15' 41"E; Fig. 1). This lagoon which has an elongated elliptic form (33 x10 km) and a major WNW-ESE axis covers an area of about 230 Km^2. It has a maximum water depth of 6m in the middle part of the basin (Guélorget et al., 1982; Medhioub, 1984). The Eastern periphery of the EBL is partially separated from the Mediterranean Sea (Gulf of Gabes) by two peninsulas namely El Gharbi (western) and Ech Chargui (eastern), each of about twelve kilometres long (Medhioub, 1979). These two peninsulas, called slobs, are cut at their mid-part by nine small islets and channels: the zone of connection with the Mediterranean waters (Medhioub & Perthuisot, 1981). The two slobs are represented by emerged Tyrrhenian aeolian littoral dunes and carbonate sand beach (Jedoui, 2000; Jedoui et al., 2002). The El Bibane Lagoon has a microtidal regime where tidal amplitude varies from 0.8 to 1.5 m (Davaud and Septfontaine, 1995; Sammari et al., 2006). The intertidal flats are flooded and exposed daily at regular intervals during the periodically rising and retreating tide. Supratidal flats are flooded at irregular intervals during spring tides or strong onshore winds (Bouougri & Porada, 2012). The El Bibane lagoon is relatively unaffected by human

activities (Pilkey, 1989; Ounalli, 2001) where it is only exploited by traditional fisheries (Guélorget et al., 1982).

3. Climate and hydrology

The southeastern Tunisia region is characterized by a pre-Saharan and arid to semi-arid climate. The hot season extends beyond the summer (Amari 1984; Ferchichi, 1996; Hamza, 2003) and the number of sunny days may reach 64.4%. The rainfall is low with an annual average that does not exceed 200 mm (Hamza, 2003). Furthermore, rainfall is very fluctuating with high inter-annual variability and intensity. Most of the rainfall is concentrated within 30 days/year (Genin and Sghaier, 2003) leading to high fluctuations in water discharge. The highest precipitation occurs mainly in October to March while in the summer months there are drought conditions.

The annual precipitations of Medenine and Tataouine stations during the last century were obtained from the Tunisian General Administration of Water Resources (DGRE, 2010, Fig.2). Five major enhanced precipitation events were recorded from these two stations (i.e. A.D 1932, A.D 1969, A.D 1979, A.D 1984 and A.D 1995). These events have induced large flood events in the Fessi River watershed (Poncet, 1970; Bonvallot, 1979; Oueslati, 1999; Boujarra and Kttita 2009; Fehri, 2014).

4. Materials and Methods

4.1. Materials

Eighteen surface sediment samples were collected from the watershed (Jerba, Zarzis, Medenine, Tataouine and Ben Guerdane localities) in order to assess the origin of the material transported into lagoon (Fig. 3). The location of all sampling stations was recorded by GPS (GPSmap 60, Garmin). The main potential sediment sources were sampled in order to characterize their sedimentological and chemical signatures as follow:

- three samples from the beach area (S1, S2 and S3) representing the marine source,

- ten samples (S7 to S16) from Fessi River catchment representing the fluvial/river sources,
- two dune samples (S17 and S18) representing the eolian component.
- three surface samples (S4 to S6) from El Bibane lagoon have been selected to represent the present-day sedimentation. S6 represents the surface sediment sample of a lagoon sediment core (BL12-10).

Moreover, to reconstruct the recent flood events occurred in the studied area, a short sediment core (BL12-10, 40 cm length; Latitude: 33°14'58.7"; Longitude: 11°10'3.7" Fig.3) was recovered from the El Bibane Lagoon (EBL) by a hand corer 75mm diameter PVC tube.

4.2. Analytical methods

4.2.1. Sedimentological and geochemical analysis

The BL12-10 core was first split, photographed and logged in detail. Elemental geochemical analyses by energy-dispersive X-ray fluorescence spectrometry were undertaken with a hand-held Niton XL3t. Measurements were realized on the watershed surface samples and each 2 cm along the BL12-10 core. BL12-10 core and surface samples had been covered with a 4µm thin Ultralene film to avoid contamination of the XRF measurement unit and the desiccation of the sediment (Richter et al., 2006). The elemental analyses from XRF measurement were performed in mining type ModCF prolene mode. These data show directly concentrations in ppm or percentage values. This is a semi-quantitative measurement. International powder standards (NIST2702 and NIST2781) were used to assess the analytical error and accuracy of measurement, which are lower than 5% for Ti, Cr, Fe, Zn, Pb, between 5 and 15% for Ca, Mn, As, Rb, Sr, and between ca. 15 and 25% for K and Co.

Laser grain-size analyses were achieved with a Beckmann-Coulter LS13320 Particle Size Analyser (Geosciences Montpellier). Grain-size analyses were performed on surface samples and the BL12-10 sequence with an average interval of 1 cm. Each sample was

primary sieved at 1 cm, suspended in deionised water and gently shaken to achieve disaggregation. Ultrasound was used to avoid particles flocculation of sediment in the fluid module of the granulometer. For each sample, a small homogeneous amount of sediment was mixed in deionized water then sieved at 1.5 mm diameter before pouring in the Fluid Module of the Particle Sizer until to obtain an optimal obscuration rate between 7 and 12% in the Fraunhofer optical cell. The time of background and sample measurement was set to 90 s and sonication was applied during the measurement of the sample in order to improve the dispersion of fine particles in the fluid. Each sample was measured twice and the good repeatability of measurement was verified according to the statistics from the international standard ISO 13320-1.

GRADISTAT program version 4.0 (Blott, 2000) was used for grain size statistical analysis. The following sample statistics are calculated using the Method of Moments in Microsoft Visual Basic programming language: mean, mode(s), sorting (standard deviation), skewness and kurtosis. Grain size parameters are calculated arithmetically, geometrically (in microns) and logarithmically (using the phi scale) (Krumbein and Pettijohn, 1938). Linear interpolation is also used to calculate statistical parameters by the Folk and Ward (1957) graphical method and derive physical descriptions (such as “very coarse sand” and “moderately sorted”).

Finally, the percentage of the granulometric classes <2µm, 2-63µm and 63-2000µm, which stand for clay, silt and sand fractions, respectively, were calculated.

4.2.2. BL12-10 core dating

Dating of sedimentary layers was carried out using ^{210}Pb and ^{137}Cs methods on a centennial timescale. The ^{137}Cs and $^{210}Pb_{ex}$ activities analyses were performed on the fraction < 150µm by gamma spectrometry using a CANBERRA Broad Energy Ge (BEGe) detector (CANBERRA BEGe 3825). The sediment was then finely crushed after drying, and

transferred into small tubes (diameter 14 mm), and stored for more than 3 weeks to ensure equilibrium between ^{226}Ra and ^{222}Rn. Generally, counting times of 24 to 48 h were required to reach a statistical error of less than 10% for $^{210}Pb_{ex}$ in the deepest samples and for the 1963 ^{137}Cs peak. Activities of ^{210}Pb were determined by integrating the area of the 46.5-keV photo-peak. ^{226}Ra activities were determined from the average of values derived from the 186.2-keV peak of ^{226}Ra and the peaks of its progeny in secular equilibrium with ^{214}Pb (295 and 352 keV) and ^{214}Bi (609 keV). In each sample, the (^{210}Pb unsupported) $_{ex}$ activities were calculated by subtracting the (^{226}Ra supported) activity from the total (^{210}Pb) activity. We then used the Constant Flux/Constant Sedimentation (CFCS) model and the decrease in $^{210}Pb_{ex}$ to calculate the sedimentation rate (Goldberg, 1963). The uncertainty of the sedimentation rate obtained by this method was derived from the standard error of the linear regression of the CFCS model.

^{137}Cs was studied on the core BL12- 10 in order to assess sediment accumulation rates and chronology of the first 30 centimetres of the core. ^{137}Cs (t1/2 = 30.1 yr) is an anthropogenic radionuclide. It entered the environment in response to atmospheric nuclear tests from 1954 to 1980 AD that induced global fallouts (the first year of atmospheric releases was 1953 AD, whereas the maximum atmospheric production is reached in 1963 AD. ^{137}Cs depth profiles have been extensively used in various environments to assess sediment accumulation rates (Nittrouer et al., 1984; He and Walling, 1996; Radakovitch et al., 1999; Frignani et al., 2004).

4.2.3 Statistical analyses

Statistical methods were applied to complete and refine the analysis. Principal Component Analysis (PCA) is widely used statistical techniques in environmental geochemistry. This multivariate approaches is used to reduce the large number of variable that result from XRF analysis. Principal Component Analysis (PCA) was applied to elements in order to distinguish the different sediment sources of surface sediments and link them to the

geochemical processes or proprieties. In the present work, the dataset contains 18 samples, each of which includes concentration of 8 elements (Ca, Sr, Fe, K, Al, Ti, Si and Zr). Data are presented in the form of elemental concentration (8 variables). In this study, a statistical analysis was performed using the STATITCF (1987) which is based on variables and it is suitable for identifying the associations of variables with a set of observations. A representation quality of the parameters (positions in the factorial plane) was then performed.

5. Results

5.1. Surface sediments

5.1.1. Sediment description: grain size and morphology

Grain size analysis and binocular observation of the surface sediment samples have permitted to characterize these three groups of sediments as follow, depending on the environmental setting: Marine, Fluvial and Aeolian sources (Fig. 4 and 5). The first group encompasses sediment samples (S1, S2 and S3) collected along the coastal zone from Jerba to Zarzis beaches and the lido of El Bibane Lagoon. In this marine area, surface sediments are composed of a mixture of coarse sub-rounded quartz grains, mollusc shells and foraminifera (Fig. 4). The grain size analysis (Table 1) of samples S1 and S2 show unimodal distributions in 169µm and 203µm, respectively indicating moderately sorted fine sand sediments (Folk, 1954; Folk and Ward, 1957; fig. 5). The sample S3 is muddy sand namely very coarse silty to coarse sand sediment with unimodal distribution in 518µm.

The second group of samples (S7, S8, S9, S10, S11, S12, S13, S14, S15 and S16) came from the El Bibane delta and the Fessi River. It is assigned as the fluvial source. Binocular observations of the samples reveal reddish-brown heterogeneous particles composed mainly of shiny angular to sub angular quartz grains. Some grains display rust colour with iron oxide (Fig. 4). Figure 5 displays that the fluvial source has a bi to multimodal distribution with two or three modes. In order to obtain the best resolution in the identification of the fluvial source,

we choose to use the sediment samples which were collected only along the River Fessi: S9, S10, S12 and S13. These surface sediment samples show a decrease in the mean grain size from upstream to downstream of the River Fessi watershed (Fig .6). The decrease in the mean grain size could be explained by a strong change of the topographic slope around Tataouine. Here, the coarser material is deposited and the finer material is transported further by the river. These finer sediments are deposited in the low plain of the river and in the El Bibane lagoon. Therefore, we suggest that S9 and S10 (collected between Tataouine and the lagoon) characterize the fluvial component in the lagoon. The grain size distribution for S9 is unimodal with a mean grain size around 96 µm indicating a moderately sorted muddy sand. The corresponding size range very coarse silty/very fine sand. Sample S10 is fine silt with trimodal distribution in 7µm, 26µm and 73µm, and poorly sorted mud sediment type. These characteristics will serve to identify the fluvial source into the lagoon.

The third group consists of two samples (S17 and S18) recovered in the Aeolian sand dunes of southern Tunisia. They are composed of homogenous dark yellow sand with angular grains; some of them are coated by iron oxide (Fig. 4). Unimodal distribution in 116µm (Table 1) characterizes the aeolien samples S17 and S18. These samples are well (S18) to very well sorted (S17) and correspond to very fine sand. The characteristics of this group will serve to identify the aeolian sand dune source.

The El Bibane Lagoon surface sediments samples S4, S5 and S6 were characterized by multimodal grain size distribution (Table 1, Fig. 5). The grain size distribution of sample S4 shows very poorly sorted sandy mud with trimodal distribution at 154µm, 31µm and 96µm, which indicates a very fine sand/very coarse silt. The sample S5 is unimodal, with a mode in 116µm. It is moderately sorted very coarse silty/fine sand sediment with a muddy sand texture (Folk, 1954; Folk and Ward, 1957). The sample S6 is very coarse silty/very fine sand sediment, with a bimodal distribution in 106µm and 429µm, poorly sorted muddy sand.

5.1.2. Distribution of major and trace elements

The spatial distribution of major and trace elements in surface sediments collected in the El Bibane lagoon and in all the area mainly along the Fessi River are displayed in figure 7.

The iron (Fe) shows its highest percentages in the Fessi River samples (0.53-1.52%). Lower values characterise the aeolian dunes (0.38-0.4%) whereas this element is totally absent in marines sediments (Table 2). This same distribution pattern is also observed for Ti, K and Al. The highest contents of these elements in the Fessi River samples contrast with the lowest ones retrieved in the marine surface sediment. Aeolian dunes are characterised by intermediate values. These four elements will thus be used as indicators of terrigenous input of material to the lagoon.

Calcium (Ca) and Strontium (Sr) in the sediment are usually associated to the carbonate fraction, which can be either of allochtonous or autochtonous origin. In the sediments, carbonates are mainly of biogenic origin. In fact, due to its compatible ionic radius, Sr can replace Ca in calcite, but remains however as trace element (Fig.7). Nevertheless, both elements show the same distribution pattern. Marine surface sediments are associated with the highest values (Ca ≈ 14, 7%; Sr ≈ 1548 ppm) whereas the lowest values and thus the lowest calcite contents are retrieved in dune samples (Ca ≈ 0.8%; Sr ≈ 52 ppm). Intermediate concentrations are associated with the Fessi River catchment (Ca ≈ 7%; Sr ≈ 150 ppm) (Table 2).

Silicon (Si) and Zircon (Zr) follow similar spatial distribution pattern (Fig. 7). Higher content of these elements are observed in the River catchment samples (Si ≈20 %; Zr ≈ 300 ppm) and in the aeolian dune samples (Si ≈33%; Zr ≈ 400 ppm), whereas marine sediments show generally lower contents (Si ≈ 10%; Zr ≈ 41 ppm) (Table 2).

5.1.3. Principal component analysis (PCA)

Application of PCA varimax rotation has permitted to identify two components that explained 83% of the total variance (Fig. 8). Factor 1 account for 64.46% of total variance. This Factor is characterized by high positive loadings for Fe, Ti, K, and Al. On the other hand, Zr and Si display a moderate positive loading and are included in factor 1. Factor 2 accounts for 17.73% of the total variance (Fig. 8). It shows positive loading for Ca, Sr, Fe and K, whereas Ti, Al, Zr and Si have negative loadings.

5.2 Core BL12-10

5.2.1 Core description and grain size analysis

The sediment sequence from El Bibane lagoon presented in this study come from the core BL12-10 recovered in the nearest part of the delta of Fessi River in May 2012 (Fig. 3). The first 30 cm of the core are made of coarse-grained layers of siliciclastic sand and shell fragments inter-bedded with organic rich dark grey fine grained sediment (mud) of clay and silt. These coarse layers are interbedded with three mud layers from 6 to 10 cm, 14 to 18 cm and 26 to 30 cm core depth (Fig. 9). The thickest fine grained layers are typically composed of clay and silt sediments. The core BL12-10 is dominated by the bimodal and trimodal grain size distributions. These distributions were labeled as very coarse silty to very fine sand, poorly to very poorly sorted, fine skewed with leptokurtic distribution (Table 3).

Our results display that these three mud layers preserved in the core are also characterized by high Fe/Ca and Ti/Ca elemental ratios (Fig. 12).

5.2.2. ^{210}Pb and ^{137}Cs dating

The measured ^{210}Pb values in the uppermost 30 cm of the BL12-10 core range from 14.5 to 0.1 mBq /g (Table 4). In general, the down core distribution of $^{210}Pb_{ex}$ values follows a relatively exponential decrease with depth and the “Constant flux: Constant Supply” (CF:CS) sedimentation model was applied. The calculated sedimentation rate (SR) is about 0.48 cm/ year. The down core ^{137}Cs activity profile (Fig. 10) shows a maximum at 18 cm depth (Table

4). We attributed this maximum to the period of maximum radionuclide fallout in the Northern Hemisphere associated with the peak of atomic weapons testing in 1963. The ^{137}Cs-derived SR (0.37 cm/ year) is lower than that of the ^{210}Pb (Fig. 10). The difference between the two methods could be explained by a change of the accumulation rate between the beginning and the last part of the 20th century.

6. Discussion

6. 1. Surface sediment grain size

The grain size classifications of surface sediments from the watershed and around the El Bibane Lagoon have permitted to discriminate the main three sediment sources (Fig. 5). Aeolian sand dune source samples show homogeneous grain size particles of quartz grains as revealed by their unimodal distribution and binocular observations. Alternatively, the fluvial transported material source is relatively heterogeneous in grain size. It is likely to have a mixture of clays, silt and quartz grains of fluvial and aeolian particles which were eroded and transported from the watershed by flood and/or sand storm. On the other hand, the marine source samples from the beach and the lido localities where predominately composed of quartz grains and shell fragments.

The El Bibane Lagoon samples S4 and S5 show obviously a mixture between the different modal distributions with at least a great contribution of fluvial source (Fig. 5). The delta of the Fessi River sample S6 grain size distribution looks more likely of the fluvial source. Furthermore, the lagoon samples showed a higher variability in the grain size due to the presence of shell fragments.

6. 2. Principal component analysis (PCA)

We used PCA to identify the main factors controlling the chemical composition of the catchment and El Bibane lagoon surface sediments and to identify different groups of common origin and process. The application of PCA varimax rotation has permitted to

identify two factors that explained 83% of the total variance (Fig.8). The high positive loadings for Fe, Ti, K, and Al on Factor 1 would indicate the dominance of alumino-silicates minerals in surface sediments (Spagnoli et al., 2008; Plewa et al., 2012). These elements are thus prevailing in the river surface samples and their granulometric distributions display that their grain sizes are in the range of clay and silt. On the other hand, Zr and Si which display a moderate positive loading in factor 1 and are high in the Aeolian surface sediments. Silicon is on one hand structural element of terrigeneous aluminosilicates, but it is also abundant as quartz grains. Therefore, the Si abundance derives from accumulation of quartz grains (Shankar et al., 1987; Nath et al., 1989). These silicates originate either from adjacent desert areas by erosion or from western Saharan dunes by storms. By contrast, the Ca and Sr carbonate related elements show a positive loading with Factor 2. Ca in the marine samples is high. The high percentage of Ca in these samples is related to both the significant presence of biogenic material, but also probably the precipitation of authigenic carbonate. These results corroborate the marine origin of these sediments as revealed by the binocular observations mainly due to the existence of shell debris and confirmed by the grain size distributions. Therefore, we suggested that the first component agreed with the fine fraction of the sediment, which is mainly composed of various types of clay minerals, usually abundant in surface sediments (De Lazzari et al., 2004). On the other hand, factor 2 (Fig. 8) provides a better definition of the relatively carbonate fraction of the sediments. Consequently, these two factors differentiated carbonates from both sand and clay sediments.

6.3. El Bibane lagoon: Main sediment sources

Geochemical parameters as well as grain size data are useful indicators for the detection of significant facies changes in the stratigraphical record (Vött et al., 2002, Zhu & Weindorf, 2009). Statistical analyses of geochemical data have permitted to characterise the different sediment sources around El Bibane lagoon. Ca, Ti and Fe elements have been

chosen in order to recognize the contribution of these sources to the surface sediments of the Lagoon. Ca displays its highest abundances in marine area and is lower in sand dunes and river samples. By contrast, Ti characterises the continental source (see section 5.1.2) and shows low contents in marine samples. On the other hand, Fe is present as a maximum in the river samples and as a trace element in marine samples. Taking into account this geographic distribution, Fe/Ca as well as Ti/Ca ratios values would be higher in the continental supply (fluvial and aeolian samples) and lower in the marine source. High Fe/Ca values due to high iron content may also reflect dominating subaerial weathering and oxidation. The Fe/Ca and Ti/Ca ratio values and the position on a Fe/Ca vs. Ti/Ca diagram (Fig. 11) of El Bibane Lagoon surface sediments (samples S4, S5 and S6) are intermediate between the marine and fluvial source. Accordingly, higher Fe/Ca and Ti/Ca ratio in the lagoon sediments would be a signal of more sediment contribution from fluvial source to the lagoon during flooding.

6.4. Identification of flood layers in the El Bibane Lagoon.

In order to identify the paleo-flood events of the El Bibane Lagoon, we applied these previously discussed proxies to BL12-10 core samples. The BL12-10 core shows 3 mud layers (clay and silt mixture) preserved in the core which seems to be flood layers, i.e., coming from fluvial incursions during intense flood events. Multiproxy analysis on these mud layers show that they are characterized by high content in clay+silt, as well as high Fe/Ca and Ti/Ca elemental ratios which represent the sedimentological signature of the River Fessi. The combination of geochemical and grain size data suggest that the BL12-10 core deposits had registered flood event. Three floods events namely FL1, FL2 and FL3 have been identified in the core (Fig. 12). FL1 deposit corresponds to a 5cm thick level of finer grained silty + clay sediment. Moreover, it shows high Ti/Ca and Fe/Ca ratio. FL2 is also interpreted as a finer grained flood and is composed of 4cm thick silty-clay sediment layer. Their geochemical composition is characterized by a high Fe/Ca and Ti/Ca ratio (Fig.12). FL2 show a good

correlation between the grain size and the geochemical proxies. FL3 is also representing another fine-grained flood which is composed of a 2.5cm thick silty-clay and their geochemical proxies reveal a good correlation with the grain size signature.

Based on our age model, FL1 would have occurred around AD 1995 ± 6 yrs (Fig. 12). This sediment deposit could correspond probably to the 1995 flood event recorded in hydrological data (Fehri, 2014) and which affected Tataouine region. This flood reached a maximum discharge of 1200 m^3/s (11 to 24 hours of heavy precipitation; Boujarra and kttita, 2009) which provoked heavy losses in human lives and agricultural goods (Boujarra and Kttita, 2009).

Using the same approach, FL2 would have occurred around AD 1970±9 yrs, i.e. between AD 1965 to 1980 (Fig. 12). Between these dates, two historical extreme flood events are known (AD.1969 and AD.1979) (24 to 48 hours of heavy rainfall for the 1969 flood event; Pias et Stuckmann, 1970 and Kallel et al.,1972; 4 days of heavy rainfall of the 1979 flood event; Bonvallot, 1979) and one flood event of lower magnitude (AD.1972). Only one horizon corresponds to these events in the BL12-10 core. Consequently, we assume that this unique flood deposit registers a period during which these three high precipitation events occurred (i.e. AD.1969, AD.1972 and AD.1979). The most suspended sediment from the river Fessi during these heavy precipitation events could have been deposited in the inundation plain, in the lagoon and probably transported to the Mediterranean Sea through the passes. The sedimentation rate corresponding to these events in the lagoon is not very high. Bottom currents in the lagoon have probably smoothed the signal. Lastly, these three extreme flood events very close together in time are registered as only one deposit in our sedimentary archive.

Finally, the third flood event FL3 was dated at A.D 1945±9 (Fig. 12). It could be associated to the 1932 flood occurrence registered in southern Tunisia historical records

(Fehri, 2014). A heavy rainfall has been recorded in Medenine region during the flood of 1932 (449 mm during few days). Bonvallot, 1979 demonstrated that this event presents a similar characteristic than that of 1979.

The results show temporal correspondence of flood layers to historical heavy precipitation events. Considering the historical data, we can assume that FL3 flood deposit corresponds to A.D 1932 flood. FL2 flood deposit is associated to A.D 1969, A.D 1972 and A.D 1969 flood events. FL1 flood deposit could be associated to the A.D 1995 flood event (Fig. 12). In this lagoonal environment, one flood deposit is not always associated to a single event but sometimes to two or three events especially when heavy precipitation events are close together in time (i.e. FL2 flood deposit).

These results indicate that finer material, high content of mud (clay+silt), as well as high ratios of Fe/Ca and Ti/Ca are associated to flood events in the lagoonal sequence. The association of these proxies in the sedimentary sequence of the El Bibane lagoon can therefore be used to reconstruct flood activities in Southeastern Tunisia during the upper Holocene.

Conclusion

This study focuses on the sedimentological and geochemical characterization of the main surface sediments sources of El Bibane Lagoon (southeast Tunisia) and its watershed in order to identify the specific signature of paleoflood events recorded in the sedimentary core archives. We used PCA to identify the main factors controlling the chemical composition of the catchment and El Bibane lagoon surface sediments and to discriminate between the sources of detrital inputs into the lagoon. Three sediments sources were identified: Aeolian, fluvial and marine. Our results display that El Bibane Lagoon surface sediment characteristics are situated between marine and river sources. The application of this multi-proxy analysis on the BL12-10 core shows that finer material, high content of mud (clay+silt), as well as high

elemental ratios (Fe/Ca and Ti/Ca) typify the sedimentological signature of flood events in the lagoonal sequence. The BL12-10 age model based on ^{210}Pb and ^{137}Cs activity profiles have allowed us to identify three periods of past flood events dated at AD 1995±6, AD 1970±9, and 1945±9. The good agreement between our estimated ages and the historical flood events suggests that sedimentological and geochemical data of lagoon sediment cores could be used to reconstruct paleoflood history in South-eastern Tunisia in arid and semi-arid environment during the upper Holocene.

Acknowledgments

Our thanks go to Dr. M. Ouaja, Ph. Blanchemache and J.P. Degai for their help on the field. We also thank Pr. Y. Jedoui and G. Siani for their fruitful suggestions in the discussions. This study is funded by the MISTRALS PALEOMEX and the PHC-UTIQUE N° 14G1002 projects.

References

Amari, A. : Contribution à la connaissance hydrologique et sédimentologique de la plateforme des îles Kerkennah Thèse de 3ème cycle. Faculté des Sciences de Tunis, Tunis, 1984.

Baker, V.R.: Magnitude and frequency of paleofloods. In: Beven, K., Carling, P. (Eds.), Floods: Hydrological, Sedimentological, and Geomorphological Implications. Wiley, Chichester, pp, 171-183, 1989.

Benito, G., Díez-Herrero, A., and Fernández de Villalta, M.: Magnitude and Frequency of Flooding in the Tagus Basin (Central Spain) over the Last Millenium', Clim. Change, 58, 171–192, 2003.

Blott, S.J.: Gradistat version 4.0 - A Grain Size Distribution and Statistics Package for the Analysis of unconsolidated sediments by Sieving or Laser Granulometer. Surface Processes and Modern Environments Research Group, Department of Geology, Royal Holloway, University of London, Egham, Surrey TW20 0EX, 2000.

Bonvallot, J.: Comportement des ouvrages de petite hydraulique dans la région de Médenine (Tunisie du Sud) au cours des pluies exceptionnelles de mars 1979, les Cahiers de l'O.R.S.T.O.M, Série Sciences Humaines XVI, 3, 233-249, 1979.

Bouaziz, S., Barrier, E., Souissi, M., Turki, M.M., and Zouari, H.: Tectonic evolution of the northern African margin in Tunisia from paleostress data and sedimentary record, Tectonophysics 357, 227-253, 2002.

Boujarra, A., and Kttita, A.: Les facteurs de l'amplification de l'inondation de la ville de Tataouine le 24 septembre 1995 (SUD EST TUNISIEN), Risques naturelles en Méditerranée occidentale, p 195-206, 2009.

Bouougri, E.H. and Porada, H.: Wind-induced mat deformation structures in recent tidal flats and sabkhas of SE-Tunisia and their significance for environmental interpretation of fossil structures, Sedimentary Geology, 263–264, 56–66, 2012.

Busson, G. : Le mésozoïque saharien 1ère partie : l'Extrême Sud tunisien. Centre National de la Recherche Scientifique, Paris, Géologie, 8, 204 p, 1967.

Brown, S.L., Bierman, P.R., Lini, A., and Southon, J.: 10 000 yr records of extreme hydrologic events. Geology, 28, 335-338, 2000.

Davaud, E. and Septfontaine, M.: Post-mortem onshore transportation of epiphytic foraminifera: recent example from the Tunisian coastline, Journal of Sedimentary Research 65, 136-142, 1995.

Degeai, J.P., Devillers, B., Dézileau, L., Oueslati, H., and Bony, G.: Major storm periods and climate forcing in the Western Mediterranean during the Late Holocene, Quaternary Science Reviews, 129, 37-56, 2015.

Dezileau, L., Sabatier, P., Blanchemanche, P., Joly, B., Swingedouw, D., Cassou, C., Castaings, J., Martinez, P., and Von Grafenstein, U.: Intense storm activity during the

Little Ice Age on the French Mediterranean coast, Palaeogeogr. Palaeocl., 299, 289-297, 2011.

Dezileau, L., Perez-Ruzafa, A., Blanchemanche, P., Martinez, P., Marcos, C., Raji, O., Van Grafenstein, U. : Extreme storms during the last 6,500 years from lagoonal sedimentary archives in Mar Menor (SE Spain), Climate of the Past, 12, 1389-1400, 2016.

De Lazzari, A., Rampazzo, G., and Pavoni, B.: Geochemistry of sediments in the Northern and Central Adriatic Sea, Estuarine, Coastal and Shelf Sciences 59, 429-440, 2004.

Direction Générale des Ressources en Eaux (DGRE): Annuaires hydrométéorologiques 1976 2010, Ministère de l'Agriculture, l'Environnement et les ressources en eau, Tunisie, 2010.

Donnelly, J. P. and Woodruff, J. D.: Intense hurricane activity over the past 5,000 years controlled by El Nino and the West African monsoon, Nature, 447, 465–468, 2007.

Ely, L.L., Enzel, Y., Baker, V.R., and Cayan, D.R.: A 5000-year record of extreme flood and climatechange in the southwestern United States. Science, 262,410–412, 1993.

Fehri, N. : L'aggravation des risques d'inondation en Tunisie : éléments de réflexion. Physio-Géo. Géographie, physique et environnement, Volume 8, 149-175, 2014.

Ferchichi, A., 1996. : Etude climatique en Tunisie présaharienne : proposition d'un nouvel indice de subdivision climatique des étages méditerranéens aride et saharien. Medit (italy), 3/96: 46-53.

Folk, R.L.: The distinction between grain size and mineral composition in sedimentary rock nomenclature. Jour. Geology 62, 344-359,1954.

Folk, R. L., and Ward, W. C.: Brazos river bar: A study in the significance of grain size parameters, Journal of Sedimentary Petrology 27, 3-26, 1957.

Frignani, M., Sorgente, D., Langone, L., Albertazzi, S., and Ravaioli, M. : Behaviour of Chernobyl radiocesium in sediments of the Adriatic Sea off the Po River delta and the Emilia-Romagna coast. J. Environ. Radioactivity 71, 299-312, 2004.

Genin, D. and Sghaier, M.: Pratiques et usages des ressources, techniques de lutte et devenir des populations rurales, Rapport scientifique final de synthèse, IRA, IRD (Projet Jeffara), 20, 2003.

Gilli, A., Anselmetti, F.S., Glur, L., and Wirth, S.B.: Lake Sediments as Archives of Recurrence Rates and Intensities of Past Flood Events, Dating Torrential Processes on Fans and Cones, Advances in Global Change Research 47, DOI 10.1007/978-94-007-4336-6 15, 2013.

Goldberg, E.: Geochronology with lead-210, International Atomic Energy Agency, 121–131, 1963.

Guélorget, O., Frisoni, G.F., and Perthuisot, J.P.: Contribution à l'étude biologique de la Bahiret el Biban : lagune du Sud-Est Tunisien, Mémoires de la Société Géologique de France 144, 173-186, 1982.

Hamza, A. : Le statut du phytoplancton dans le golfe de Gabès. Thèse de Doctorat, Université de Sfax, 298, 2003.

He and Walling.: Use of fallout Pb-210 measurements to investigate longer-term rates and patterns of overbank sediment deposition on the floodplains of lowland rivers Earth Surf. Proc. Land., 21 pp. 141–154, 1996.

Jedoui, Y. : Sédimentologie et géochronologie des dépôts littoraux quaternaires: reconstitution des variations des paléoclimats et du niveau marin dans le Sud-Est tunisien. Thèse d'Etat es. Sciences., Fac. Sc. Tunis, Université de Tunis El Manar, 338, 2000.

Jedoui, Y., Kallel, N., Fontugne, M., Ben Ismail, M.H., M'Rabet, A., and Montacer, M.: A

relative sea-level stand in the middle Holocene of southeastern Tunisia: Marine Geology., 147, 123–130, 1998.

Jedoui, Y., Davaud, E., Ben Ismaïl, H,. and Reyss, J.L.: Analyse sédimentologique des dépôts marins pléistocènes du Sud-Est tunisien: mise en évidence de deux périodes de haut niveau marin pendant le sous-stade isotopique marin 5e (Eémien, Tyrrhénien), Bulletin de la Société Géologique de France 173, 63-72, 2002.

Kallel, R., Colombani, J., Eoche duval, J.M. : Les précipitations et les crues exceptionnelles de l'automne 1969 en Tunisie, publication de la division des ressources en eau, Ressouces en eau de Tunisie, 1972.

Krumbein, W.C. and Pettijohn, F.J.: Manual of Sedimentary Petrography. Appleton-Century-Crofts, New York, 1938.

Lionello, P., Bhend, J., Buzzi, A., Della-Marta, P., Krichak, S., Jansa, A., Maheras, P., Sanna, A., Trigo, I., and Trigo, R.: Cyclones in the Mediterranean region: climatology and effects on the environment, Developments in Earth and Environmental Sciences, 4, 325–372, 2006.

Liu, K.B. and Fearn, M. L.: Lake-sediment record of late Holocene hurricane activities from coastal Alabama, Geology, 21, 793– 796, 1993.

Medhioub, K. : La Bahiret El Bibane. Etude géochimique et sédimentologique d'une lagune du Sud-Est tunisien, Travail du laboratoire de Géologie, Presse de l'école Normale Supérieure, Paris, 13, 150, 1979.

Medhioub, K. : Etude géochimique et sédimentologique du complexe paralique de la dépression de ben Guirden: Bahira el Biban, Sabkha bou J'Mel et Sabkha el Medina. Thèse Doctorat es- Sciences, Ecole Normale Supérieur, Paris, 400, 1984.

Medhioub, K.and Perthuisot, J.P.: The influence of peripheral sabkhas on the geochemistry and sedimentology of a Tunisian lagoon: Bahiret el Biban, Sedimentology, 28, 679–688. 1981.

Mejri, F., Burollet, P.F., and Ben Ferjani, A.: Petroleum geology of Tunisia: A renewed synthesis, Memoir ETAP 22, 233, 2006.

Moreno, A., Valero-Garcés, B., Gonzales-Sampériz, P., and Rico, M.: Flood response to rainfall variability during the last 2000 years inferred from the Taravilla Lake record (Central Iberian Range, Spain). Journal of Paleolimnology 40, 943–961, 2008.

Nath, B.N., Rao, V.P., and Becker, K.P.: Geochemical evidence of terrigenous influence in deep-sea sediments up to 8° S in the central Indian basin, Marine Geology., 87, 301-313. 1989.

Nittrouer, C.A., DeMaster, D.J., Kuehl, S.A., McKee, B.A., Thorbjarnarson, K.W.: Some questions and answers about the accumulation of fine-grained sediments in continental margin environments. Geo-Marine Letters, 4, 211-213. 1984- 1985

Ounalli, A. : Projet de dessalement d'eau de mer à El Bibane. Desalination, 137, 293-296, 2001.

Oueslati, A.: Les inondations en Tunisie. Publication à compte d'auteur, p. 206, 1999.

Parris, A.S., Bierman, P.R., Noren, A.J., Prins, M.A., Lini, A.: Holocene paleostorms identified by particle size signatures in lake sediments from the northeastern United States, J. Paleolimnol 43,29–49, 2009.

Poncet, J.: La catastrophe climatique de l'automne 1969 en Tunisie, Annales de Géographie, vol 79, n°435, p.581-595,1970.

Pias, J.and Stuckmann, G.: Les inondations de septembre- octobre 1969 en Tunisie, Partie 2 Etude morphologique, UNESCO, Paris, 1970.

Pilkey, O.H.: A thumbnail method for beach communities: estimation of long-term beach

replenishment requirements, Shore and Beach, July, 1988. 23 - 31. 1989.

Plewa, K., Meggers, H., Kuhlmann, H., Freudenthal, T., Zabel, M., and Kasten, S.: Geochemical distribution patterns as indicators for productivity and terrigenous input off NW Africa. Deep Sea Research, I 66, 51-66, 2012.

Raji, O., Dezileau, L., Von Grafenstein, U., Niazi, S., Snoussi, M., and Martinez, P.: Sea extreme events during the last millennium in north-east of Morocco, Natural. Hazards Earth, Systems Science Discussion, 2, 2079-2102, 2014.

Raji, O.: Evénements extrêmes du passé et paleo-environnements: reconstruction à partir des archives sédimentaires de la lagune Nador, Maroc, Thèse de Doctorat, Université Mohammed V de Rabat. 2014.

Radakovitch, O., Charmasson, S., Arnaud, M., Bouisset, and P.: 210Pb and caesium accumulation in the Rhône delta sediments. Estuar. Coast. Shelf Sci 48, 77–92. 1999.

Richter, T.O., Van der Gaast, S., Koster, B., Vaars, A., Gieles, R., de Stigter, H.C., De Haas, H., and Van Weering, T.C.E.: The Avaatech XRF Core Scanner: technical description and applications to NE Atlantic sediments, In: Rothwell, R.G. (Eds.), Techniques in Sediment Core Analysis: Geological Society of London, Special Publications, 39–50. 2006.

Sabatier, P., Dezileau, L., Condomines, M., Briqueu, L., Colin, C., Bouchette, F., Le Duff, M., and Blanchemanche, P.: Reconstruction of paleostorm events in a coastal lagoon (Herault, South of France), Marine Geol., 251, 224–232, 2008.

Sammari, C., Koutitonsky, V.G., Moussa, M.: Sea level variability and tidal resonance in the Gulf of Gabes, Tunisia, Continental Shelf Research, 26, 338-350, 2006.

Shankar R., Subarrao, K.V., and Kolla, V.: Geochemistry of surface sediments from the Arabian Sea. Marine Geology, 76, 253-279, 1987.

Spagnoli, F., Bartholinia, G., Dinelli, E., and Giordano, P.: Geochemistry and particle size of surface sediments of Gulf of Manfredonia (Southern Adriatic Sea), Estuarine, Coastal and Shelf Science 80, 21–30,2008.

St. George, S and E. Nielson.: Paleoflood records for the Red River, Manitoba, Canada, derived from anatomical tree-ring signatures: The Holocene 13 (4), 547-555, 2003.

STATIT-CF: Services des études statistiques de l'I.T.C.F.

Vött, A., Handl, M. and Brückner, H. Rekonstruktion holozäner Umweltbedingungen in Akarnanien (Nordwestgriechenland) mittels Diskriminanzanalyse von geochemischen Daten. Geologica et Palaeontologica 36: 123-147, 2002.

Wilhelm, B., Arnaud, F., Sabatier, P., Crouzet, Ch., Elodie, B., Eric, Ch., Jean-Robert, D., Frederic, G., Emmanuel, M., Jean-Louis, R., Kazuyo,T., Edouard, B., and Jean-Jacques, D.: 1400 years of extreme precipitation patterns over the Mediterranean French Alps and possible forcing mechanisms, Quaternary Research; 78, 1-12, 2012.

Wolfe, B.B., Hall, R.I., Last, W.M., Edwards, T.W.D., English, M.C., Karst-Riddoch, T.L., Paterson, A., and Palmini, R.: Reconstruction of multi-century flood histories from oxbow lake sediments, Peace-Athabasca Delta, Canada. Hydrol. Process, 20, 4131- 4153, 2006.

Zielhofer, C., Faust, D., Baena, R., Diaz del Olmo, F., Kadereit, A., Moldenhauer, K.-M., Porras, A.: Centennial-scale late Pleistocene to mid-Holocene synthetic profile of the Medjerda floodplain (Northern Tunisia). The Holocene 14, 851–861, 2004.

Zhu, Y. & Weindorf, D.: Determination of soil calcium using field portable X-ray fluores-cence. Soil Science, 174 (3), 151-155, 2009.

Figures

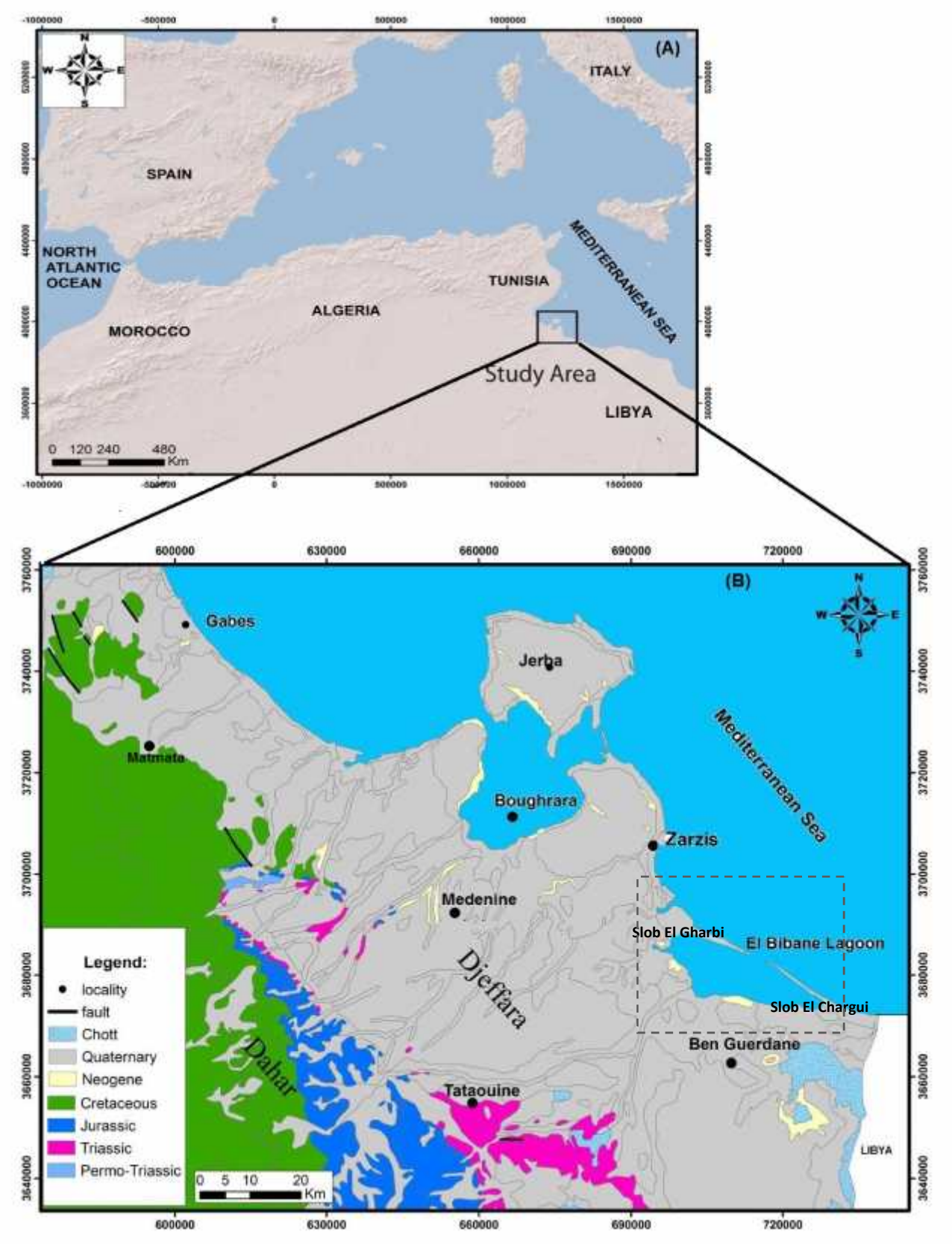
(A)
ITALY
SPAIN
NORTH ATLANTIC OCEAN
MEDITERRANEAN SEA
TUNISIA
ALGERIA
MOROCCO
Study Area
LIBYA
0 120 240 480 Km
(B)
Gabes
Jerba
Matmata
Boughrara
Mediterranean Sea
Zarzis
Medenine
Slob El Gharbi
El Bibane Lagoon
Djeffara
Slob El Chargui
Dahar
Ben Guerdane
Tataouine
LIBYA
Legend:
locality
fault
Chott
Quaternary
Neogene
Cretaceous
Jurassic
Triassic
Permo-Triassic
0 5 10 20 Km

1

Figure.1. Location of the study area of El Bibane Lagoon (EBL) South East of Tunisia (A) and the geological map of South Eastern Tunisia (Modified from the Geological map of Tunisia 1/500000 after Ben Haj Ali et al., 1985) (B).

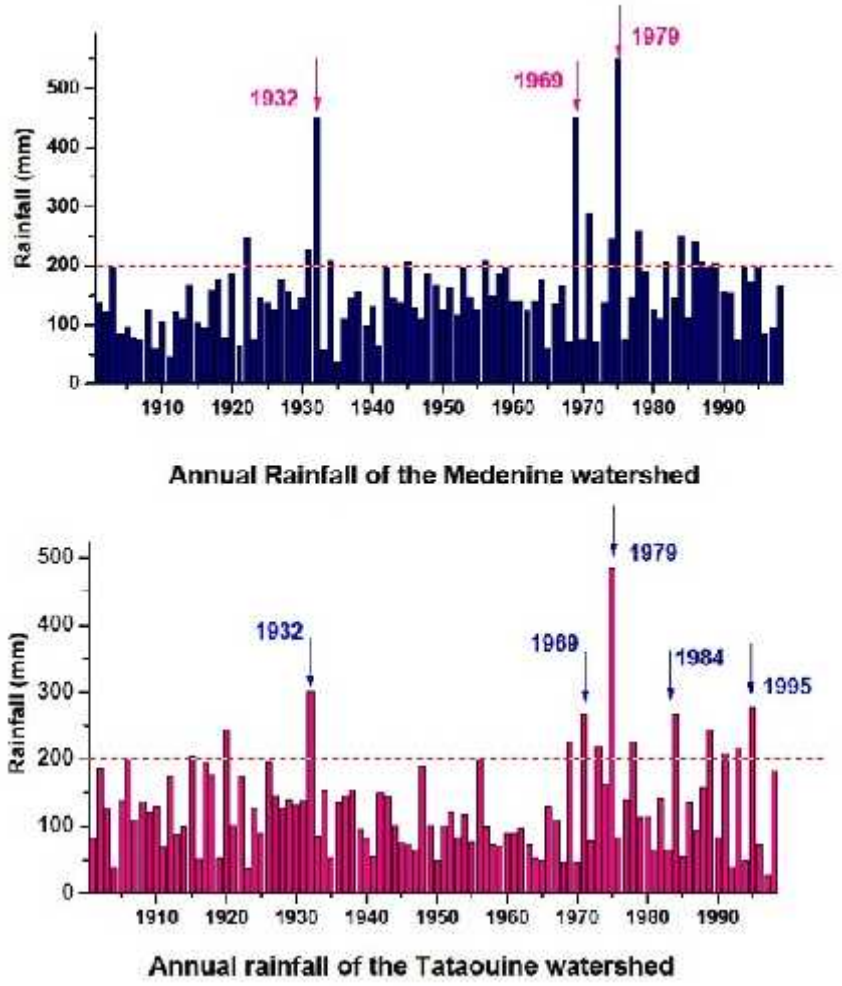

Figure.2. Variation of the annual precipitations of the Medenine and Tataouine meteorological stations during the period between 1900 and 2000 (DGRE, 2010). Dashed line: mean annual precipitation.

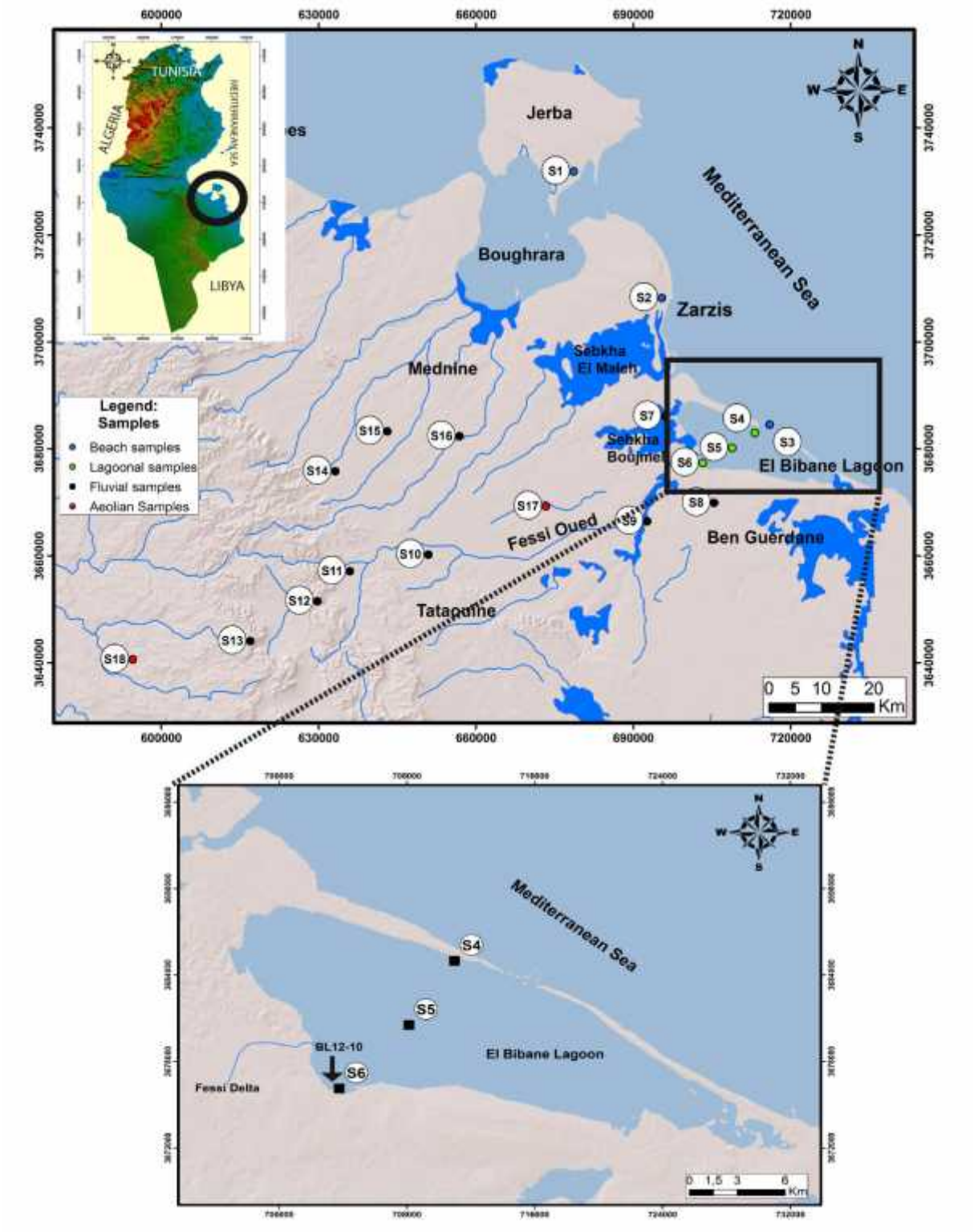

Figure.3. Location of the investigated surface samples from the catchment basin and from the El Bibane Lagoon.

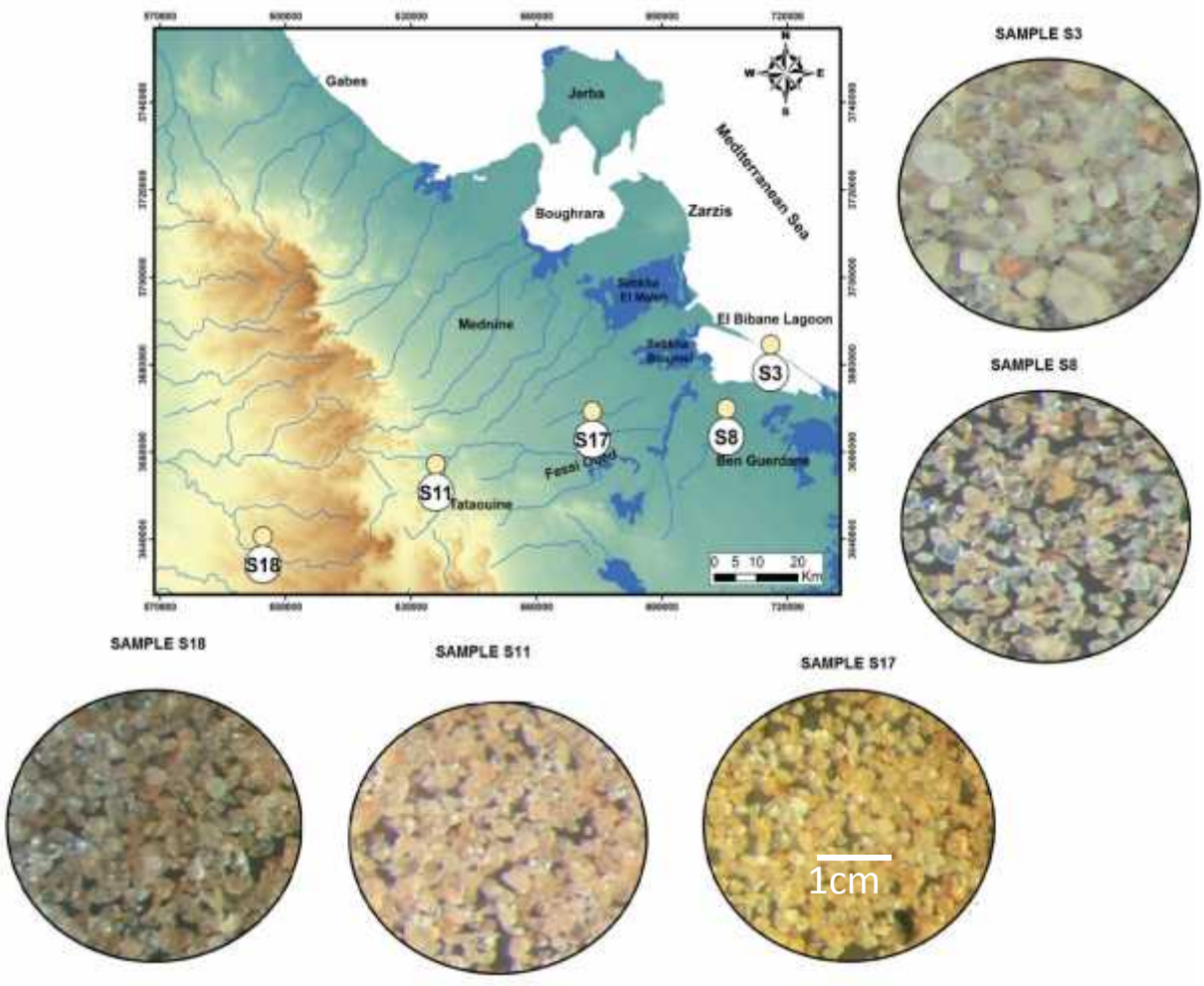

Figure.4. Microtextural photos under binocular observation of five representative samples from the catchment basin of El Bibane Lagoon. S3 Marine sample; S8 and S11: Fessi River samples; S17 and S18: Dunes samples (Diameter of the photos: 3 cm; G x 6.5).

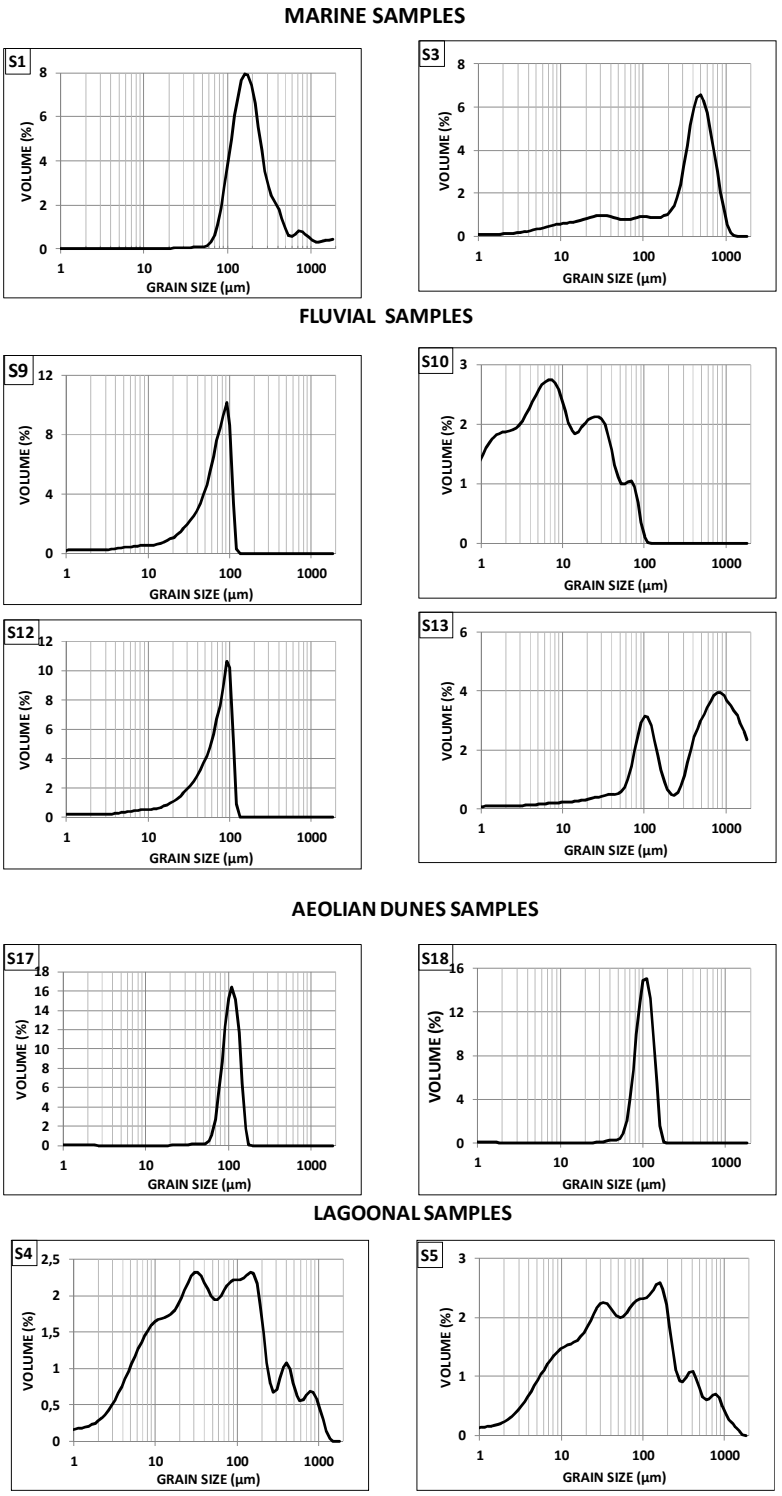

Figure.5. Particle size distributions (<2000µm) of representative samples from the catchment basin and the El Bibane Lagoon.

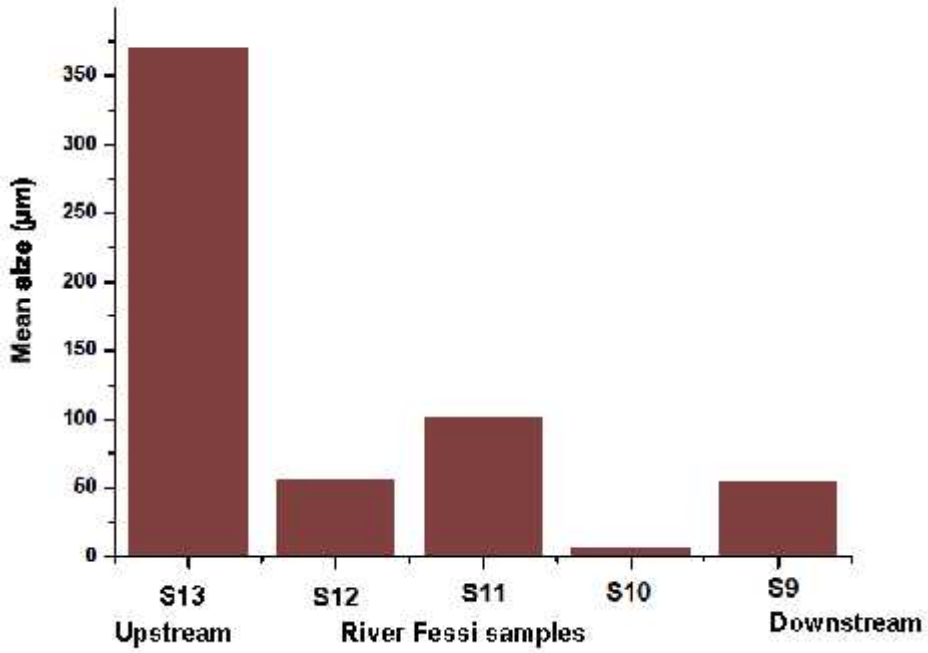

Figure.6: Distribution of the mean size of the samples collected in the Fessi River

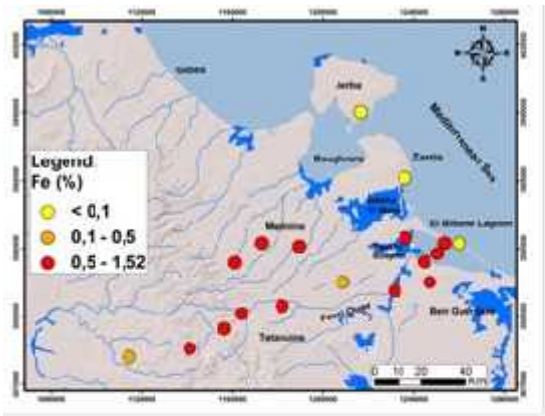
Legend
Fe (%)
< 0,1
0,1 - 0,5
0,5 - 1,52

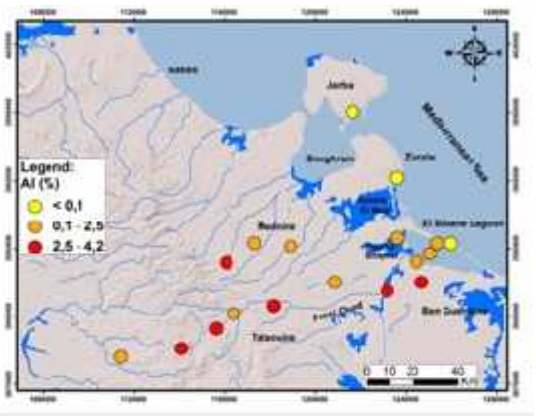
Legend:
Al (%)
< 0,1
0,1 - 2,5
2,5 - 4,2

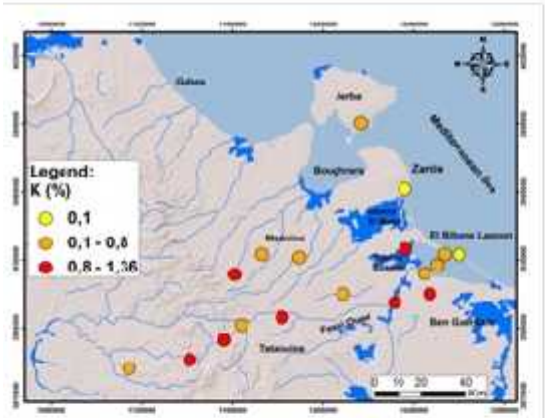
Legend:
K (%)
0,1
0,1 - 0,8
0,8 - 1,36

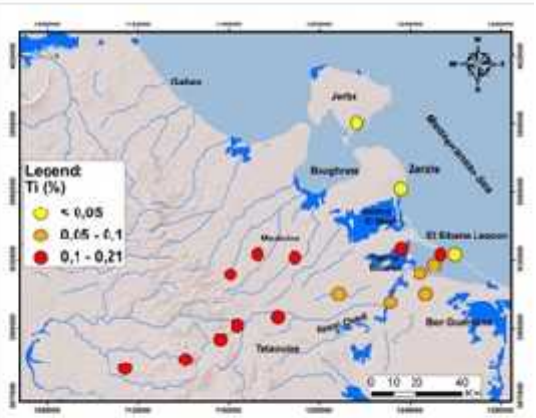
Legend:
Ti (%)
< 0,05
0,05 - 0,1
0,1 - 0,21

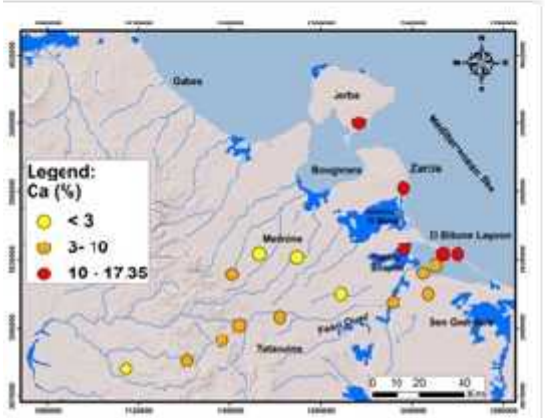
Legend:
Ca (%)
< 3
3- 10
10 - 17 35

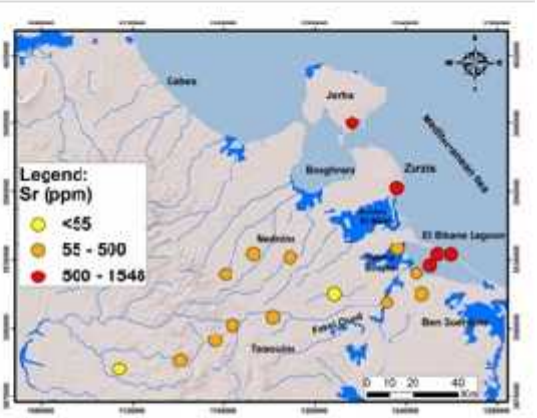
Legend:
Sr (ppm)
<55
55 - 500
500 - 1546

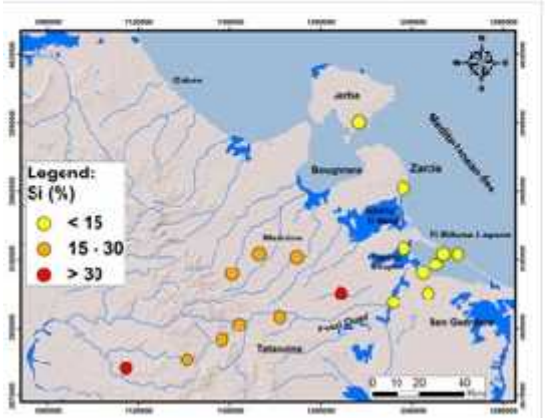
Legend:
Si (%)
< 15
15 - 30
> 30

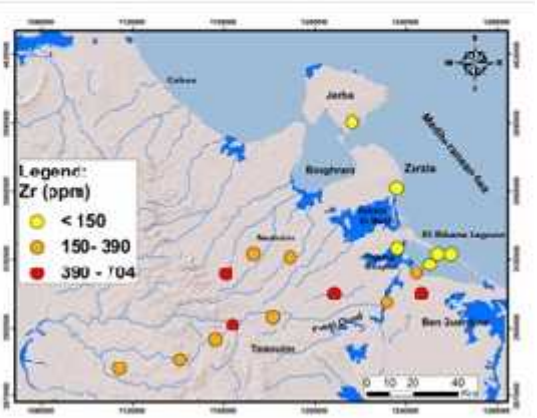
Legend:
Zr (ppm)
< 150
150- 390
390 - 704

1

Figure.7. Distribution map of major and trace elements in surface sediments from catchment basin and the El Bibane lagoon.

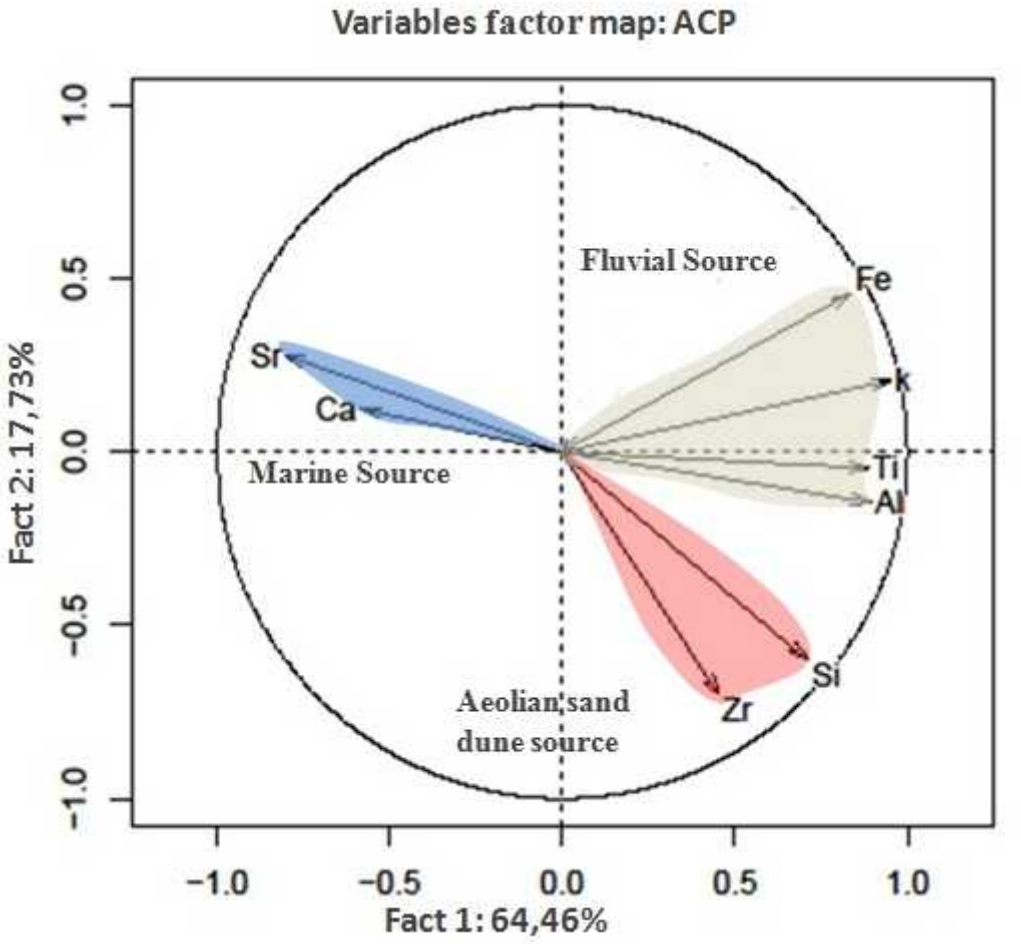

Figure.8. Principal Component Analysis (PCA) loadings plot of major and trace elements concentrations contrasting the three main sources: marine, fluvial and a eolian sand dune.

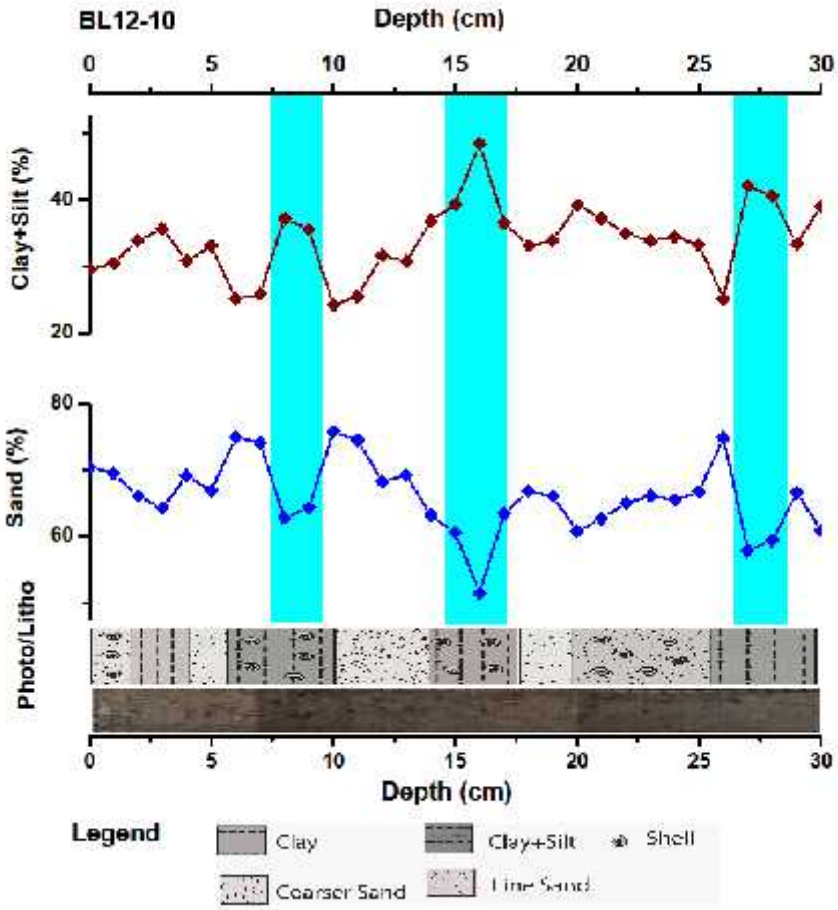

1

2

3 Figure.9. Sand and silt+ clay fractions depth profiles in core BL12-10.

4

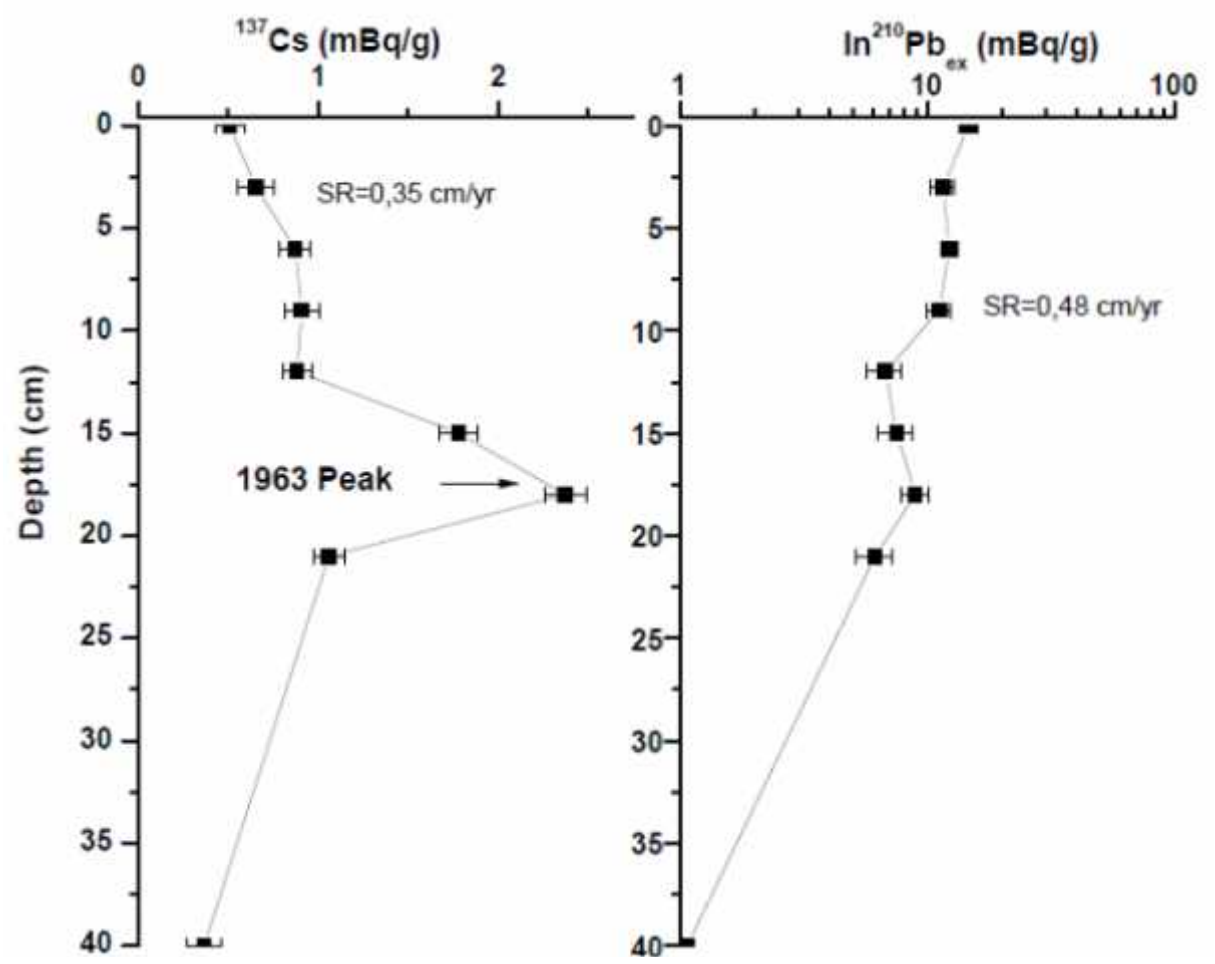

Figure.10. $^{210}Pb_{ex}$ and ^{137}Cs activity-depth profiles in core BL12-10. SR: sedimentation rate (cm yr^{-1})

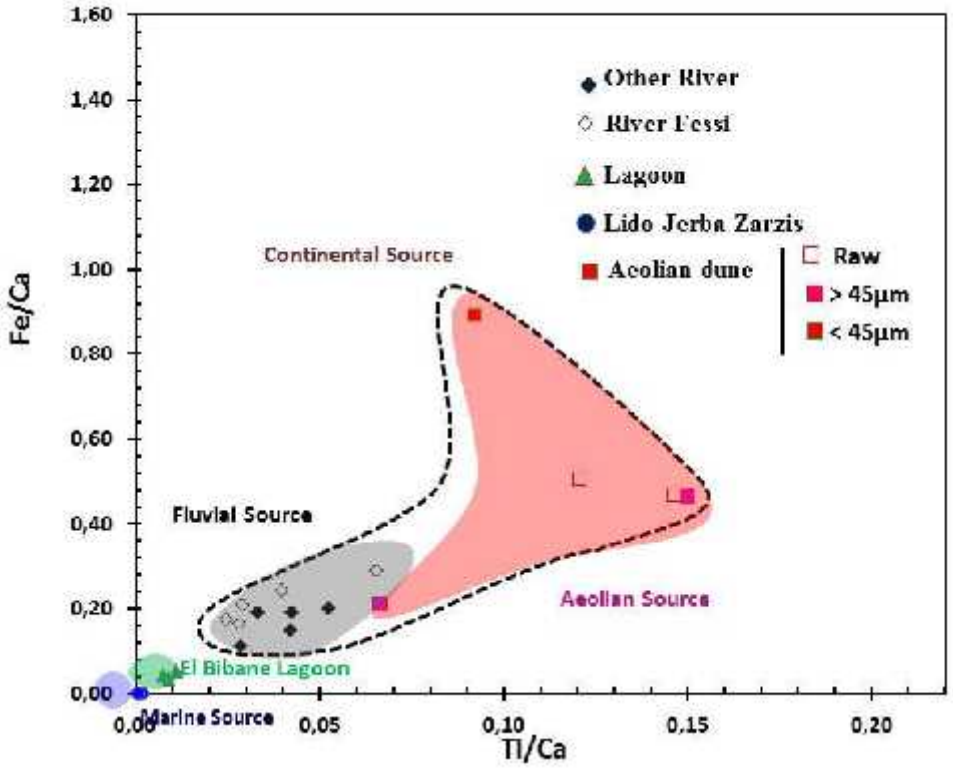

Figure.11. Location of the investigated surface samples from the watershed and the El Bibane Lagoon on a cross-plot Fe/Ca *versus* Ti/Ca.

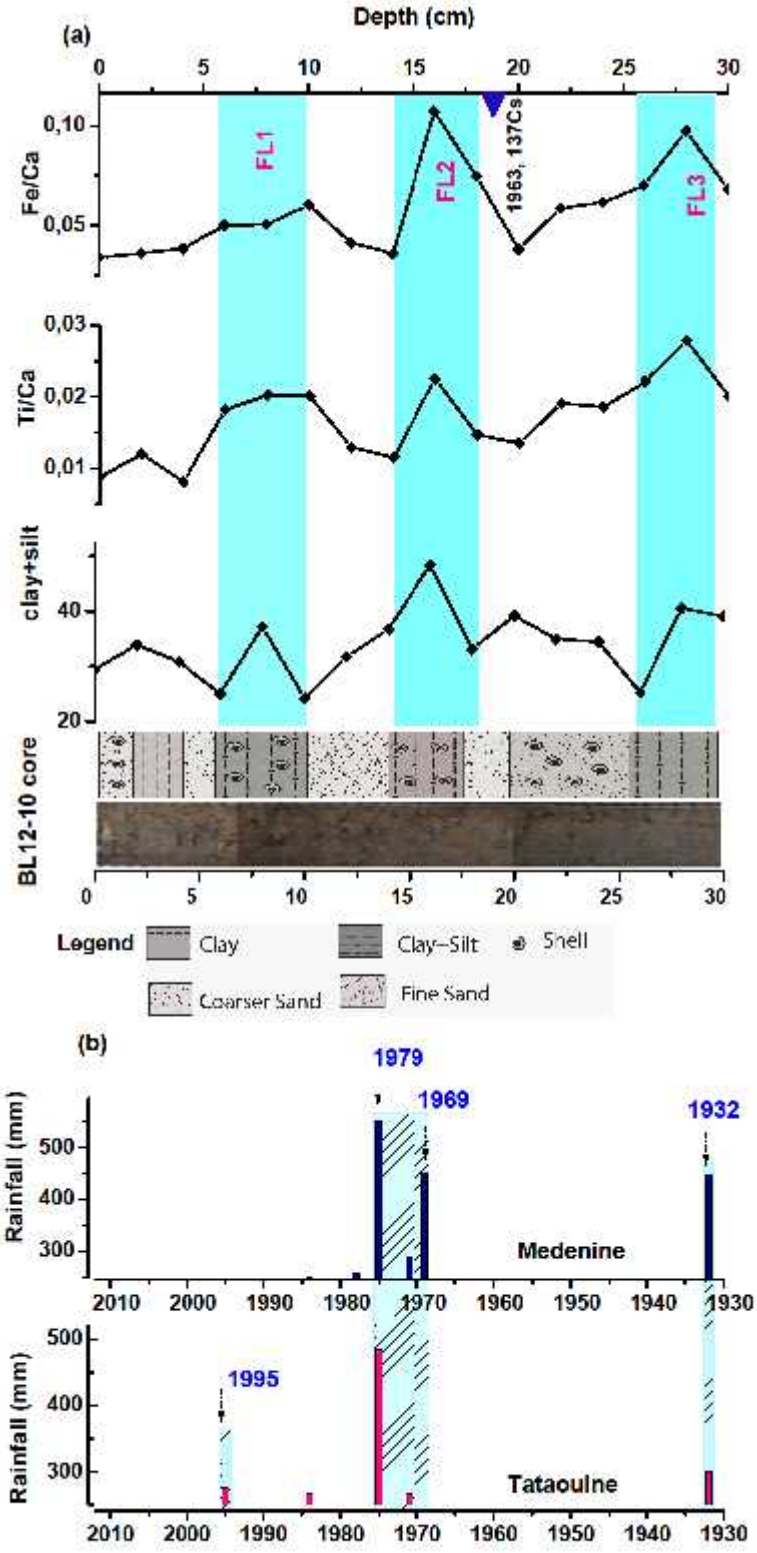

1

2 Figure.12. Fe/Ca and Ti/Ca ratios, clay + silt (fraction <63µm) abundances (%) profiles, ^{137}Cs

3 ages in the BL12-10 core (a) and their equivalent last century historical rainfall of the

Tataouine and Medenine stations (b see fig. 2). Three periods of high rainfall were observed at A.D 1932, A.D 1969/1979 and A.D 1995. FL1, FL2 and FL3 represent flood deposits registered in the sediments archive of the El Bibane Lagoon

Tables

Table 1. Grain size statistical analysis of surface samples from the watershed of the El Bibane Lagoon.

Sample name	Sampling Locality	SAMPLE TYPE	TEXTURAL GROUP	SEDIMENT NAME
S1	Beach	Unimodal, Moderately Sorted	Sand	Moderately Sorted Fine Sand
S2		Unimodal, Moderately Sorted	Sand	Moderately Sorted Fine Sand
S3		Unimodal, Very Poorly Sorted	Muddy Sand	Very Coarse Silty Coarse Sand
S4	Surface sediments El Bibane Lagoon	Polymodal, Very Poorly Sorted	Sandy Mud	Very Fine Sandy Very Coarse Silt
S5		Unimodal, Moderately Sorted	Muddy Sand	Very Coarse Silty Fine Sand
S6		Bimodal, Poorly Sorted	Muddy Sand	Very Coarse Silty Very Fine Sand
S9	Fessi River	Unimodal, Poorly Sorted	Muddy Sand	Very Coarse Silty Very Fine Sand
S10		Trimodal, Poorly Sorted	Mud	Fine Silt
S11		Unimodal, Well Sorted	Sand	Well Sorted Very Fine Sand
S12		Unimodal, Poorly Sorted	Muddy Sand	Very Coarse Silty Very Fine Sand
S13		Bimodal, Poorly Sorted	Muddy Sand	Very Coarse Silty Coarse Sand
S17	Sand dune	Unimodal, Very Well Sorted	Sand	Very Well Sorted Very Fine Sand
S18		Unimodal, Well Sorted	Sand	Well Sorted Very Fine Sand

Table 1. Continued

	FOLK AND WARD METHOD (µm)						
Sample name	**MEAN**	**SORTING**	**SKEWNESS**	**KURTOSIS**	**MODE 1 (µm)**	**MODE 2 (µm)**	**MODE 3 (µm)**
S1	196.2	1.793	0.234	1.308	169.1		
S2	249.1	1.808	0.181	1.108	203.7		
S3	204.2	4.233	-0.658	1.027	517.8		
S4	43.46	4.683	-0.027	0.931	154.0	31.54	96.60
S5	112.5	1.813	-0.221	1.203	116.4		
S6	80.39	3.156	-0.246	1.701	106.0	429.7	
S9	54.69	2.237	-0.569	1.490	96.60		
S10	7.133	3.891	0.001	0.845	7.092	26.17	73.02
S11	102.5	1.343	-0.245	1.218	116.4		
S12	56.17	2.248	-0.573	1.421	96.60		
S13	370.9	3.902	-0.410	0.883	825.4	106.0	

S17	110.5	1.260	-0.127	1.008	116.4	
S18	106.4	1.286	-0.132	1.039	116.4	

Table.2. XRF analysis results of the major and trace element in studied samples. ppm: parts per million.

Sample name	Locality	Zr (ppm)	Sr (ppm)	Ca (%)	Fe (%)	Ti (%)	K (%)	Al (%)	Si (%)
S1	Beach	113	1497	14.67	0.00	0.03	0.14	0.00	9.71
S2	Beach	41	1548	14.51	0.00	0.01	0.10	0.00	6.85
S3	Beach	24	899	13.36	0.00	0.01	0.10	0.00	8.38
S4	Lagoon	133	1035	17.35	0.75	0.13	0.74	0.40	15.00
S5	Lagoon	85	747	9.00	0.47	0.10	0.47	0.18	8.70
S6	Lagoon	203	418	7.90	0.27	0.07	0.56	0.69	12.00
S7	River	134	358	17.35	0.75	0.13	1.10	2.08	15.00
S8	River	488	90	9.00	0.53	0.10	0.81	2.60	8.70
S9	River	178	97	7.90	0.98	0.07	1.13	2.76	12.00
S10	River	235	105	7.30	1.52	0.21	1.36	4.20	26.16
S11	River	704	92	6.00	0.59	0.16	0.56	2.20	26.93
S12	River	275	173	7.37	1.22	0.21	1.12	3.60	27.43
S13	River	391	123	7.35	1.28	0.18	0.93	2.60	27.13
S14	River	458	186	7.16	0.79	0.20	0.87	2.70	26.18
S15	River	350	102	3.95	0.59	0.17	0.77	2.40	29.08
S16	River	263	73	3.22	0.62	0.11	0.74	1.80	25.62
S17	Aeolian	473	52	0.80	0.40	0.10	0.75	2.50	33.38
S18	Aeolian	357	54	0.81	0.38	0.12	0.74	2.40	33.09

Table 3. Grain size statistical analysis of BL12-10 core samples

DEPTH (cm)	Sample name	SAMPLE TYPE	TEXTURAL GROUP	SEDIMENT NAME
1	**BL12-10-1**	Bimodal, Poorly Sorted	Muddy Sand	Very Coarse Silty Very Fine Sand
2	**BL12-10-2**	Trimodal, Very Poorly Sorted	Muddy Sand	Very Coarse Silty Very Fine Sand
3	**BL12-10-3**	Trimodal, Poorly Sorted	Muddy Sand	Very Coarse Silty Very Fine Sand
4	**BL12-10-4**	Trimodal, Very Poorly Sorted	Muddy Sand	Very Coarse Silty Very Fine Sand
5	**BL12-10-5**	Trimodal, Poorly Sorted	Muddy Sand	Very Coarse Silty Very Fine Sand
6	**BL12-10-6**	Trimodal, Poorly Sorted	Muddy Sand	Very Coarse Silty Very Fine Sand
7	**BL12-10-7**	Trimodal, Poorly Sorted	Muddy Sand	Very Coarse Silty Very Fine Sand
8	**BL12-10-8**	Bimodal, Poorly Sorted	Muddy Sand	Very Coarse Silty Very Fine Sand
9	**BL12-10-9**	Bimodal, Poorly Sorted	Muddy Sand	Very Coarse Silty Very Fine Sand
10	**BL12-10-10**	Trimodal, Poorly Sorted	Muddy Sand	Very Coarse Silty Very Fine Sand
11	**BL12-10-11**	Trimodal, Poorly Sorted	Muddy Sand	Very Coarse Silty Very Fine Sand
12	**BL12-10-12**	Trimodal, Very Poorly Sorted	Muddy Sand	Very Coarse Silty Very Fine Sand

13	**BL12-10-13**	Trimodal, Poorly Sorted	Muddy Sand	Very Coarse Silty Very Fine Sand
14	**BL12-10-14**	Trimodal, Very Poorly Sorted	Muddy Sand	Very Coarse Silty Very Fine Sand
15	**BL12-10-15**	Trimodal, Poorly Sorted	Muddy Sand	Very Coarse Silty Very Fine Sand
16	**BL12-10-16**	Trimodal, Very Poorly Sorted	Muddy Sand	Very Coarse Silty Very Fine Sand
17	**BL12-10-17**	Trimodal, Very Poorly Sorted	Muddy Sand	Very Coarse Silty Very Fine Sand
18	**BL12-10-18**	Trimodal, Very Poorly Sorted	Muddy Sand	Very Coarse Silty Very Fine Sand
19	**BL12-10-19**	Trimodal, Very Poorly Sorted	Muddy Sand	Very Coarse Silty Very Fine Sand
20	**BL12-10-20**	Bimodal, Poorly Sorted	Muddy Sand	Very Coarse Silty Very Fine Sand
21	**BL12-10-21**	Bimodal, Poorly Sorted	Muddy Sand	Very Coarse Silty Very Fine Sand
22	**BL12-10-22**	Trimodal, Poorly Sorted	Muddy Sand	Very Coarse Silty Very Fine Sand
23	**BL12-10-23**	Trimodal, Poorly Sorted	Muddy Sand	Very Coarse Silty Very Fine Sand
24	**BL12-10-24**	Bimodal, Poorly Sorted	Muddy Sand	Very Coarse Silty Very Fine Sand
25	**BL12-10-25**	Trimodal, Poorly Sorted	Muddy Sand	Very Coarse Silty Very Fine Sand
26	**BL12-10-26**	Trimodal, Poorly Sorted	Muddy Sand	Very Coarse Silty Very Fine Sand
27	**BL12-10-27**	Trimodal, Very Poorly Sorted	Muddy Sand	Very Coarse Silty Very Fine Sand
28	**BL12-10-28**	Trimodal, Very Poorly Sorted	Muddy Sand	Very Coarse Silty Very Fine Sand
29	**BL12-10-29**	Trimodal, Poorly Sorted	Muddy Sand	Very Coarse Silty Very Fine Sand
30	**BL12-10-30**	Bimodal, Poorly Sorted	Muddy Sand	Very Coarse Silty Very Fine Sand

Table 3. continued.

		FOLK AND WARD METHOD (µm)						
DEPTH (Cm)	**Sample name**	**MEAN**	**SORTING**	**SKEWNESS**	**KURTOSIS**	**MODE 1 (µm)**	**MODE 2 (µm)**	**MODE 3 (µm)**
1	**BL12-10-1**	83.47	3.322	-0.179	1.633	106.0	429.7	-----
2	**BL12-10-2**	78.84	4.101	-0.173	1.438	106.0	429.7	825.4
3	**BL12-10-3**	73.43	3.905	-0.239	1.302	106.0	429.7	825.4
4	**BL12-10-4**	93.13	4.060	-0.120	1.440	106.0	391.4	825.4
5	**BL12-10-5**	83.41	3.989	-0.171	1.362	106.0	391.4	825.4
6	**BL12-10-6**	105.8	3.491	-0.099	1.687	106.0	391.4	751.9
7	**BL12-10-7**	104.5	3.591	-0.055	1.795	106.0	429.7	825.4
8	**BL12-10-8**	68.15	3.817	-0.262	1.278	106.0	429.7	-----
9	**BL12-10-9**	68.85	3.797	-0.239	1.451	106.0	429.7	-----
10	**BL12-10-10**	124.1	3.860	0.001	1.451	106.0	429.7	825.4
11	**BL12-10-11**	116.0	3.969	-0.050	1.460	106.0	391.4	825.4
12	**BL12-10-12**	100.0	4.323	-0.080	1.275	106.0	429.7	825.4
13	**BL12-10-13**	95.97	3.921	-0.098	1.452	106.0	429.7	825.4
14	**BL12-10-14**	81.56	4.213	-0.124	1.282	106.0	429.7	825.4
15	**BL12-10-15**	67.56	3.879	-0.201	1.328	106.0	429.7	825.4
16	**BL12-10-16**	51.25	4.110	-0.212	1.130	96.60	429.7	825.4
17	**BL12-10-17**	90.27	4.755	-0.080	1.155	106.0	429.7	825.4
18	**BL12-10-18**	95.70	4.271	-0.078	1.288	106.0	429.7	825.4
19	**BL12-10-19**	89.09	4.107	-0.109	1.296	106.0	429.7	825.4

20	**BL12-10-20**	65.02	3.779	-0.259	1.250	106.0	429.7	-----
21	**BL12-10-21**	68.97	3.463	-0.235	1.387	106.0	429.7	-----
22	**BL12-10-22**	79.14	3.994	-0.160	1.366	106.0	429.7	825.4
23	**BL12-10-23**	77.19	3.736	-0.196	1.448	106.0	429.7	825.4
24	**BL12-10-24**	74.94	3.526	-0.226	1.408	106.0	429.7	-----
25	**BL12-10-25**	82.29	3.753	-0.160	1.415	106.0	429.7	825.4
26	**BL12-10-26**	126.4	3.867	-0.028	1.262	106.0	391.4	751.9
27	**BL12-10-27**	66.68	4.242	-0.172	1.157	106.0	391.4	825.4
28	**BL12-10-28**	67.57	4.017	-0.198	1.216	106.0	429.7	825.4
29	**BL12-10-29**	84.27	3.865	-0.154	1.393	106.0	429.7	825.4
30	**BL12-10-30**	63.32	3.673	-0.262	1.390	106.0	429.7	-----

Table.4. Activities of radionuclides ^{210}Pb, ^{137}Cs and ^{226}Ra in core BL12-10.

Depth (cm)	**^{226}Ra (dpm/g)**			**^{210}Pb (mbq/g)**			**^{137}Cs (mbq/g)**		
0	0,586	±	0,007	14,584	±	1,157	0,507	±	0,081
3	0,556	±	0,009	11,486	±	1,202	0,655	±	0,098
6	0,592	±	0,008	12,142	±	0,924	0,872	±	0,085
9	0,574	±	0,008	11,066	±	1,221	0,908	±	0,096
12	0,596	±	0,008	6,729	±	1,048	0,883	±	0,080
15	0,598	±	0,003	7,466	±	1,175	1,782	±	0,104
18	0,582	±	0,008	8,877	±	1,103	2,375	±	0,115
21	0,592	±	0,005	6,110	±	1,005	1,060	±	0,084
40	0,659	±	0,011	1,058	±	1,476	0,365	±	0,101